REDUCED NONLINEAR MODEL OF A SPAR-MOUNTED FLOATING WIND TURBINE

Frank Sandner[1], David Schlipf[1], Denis Matha[1], Robert Seifried[2], Po Wen Cheng[1]
[1]Stuttgart Wind Energy; [2]Institute of Engineering and Computational Mechanics
University of Stuttgart, Germany
+49 (0)711 685-68 332, sandner@ifb.uni-stuttgart.de

Summary

Floating offshore wind turbines (FOWTs) are complex dynamic systems requiring a thorough design for optimal operating performance and stability. Advanced control strategies, like model predictive control, are part of the integrated development of new concepts. This paper presents a simplified and computationally efficient model of the spar-mounted OC3-Hywind FOWT. Applications are, e.g., the real-time integration within the controller or an assessment during conceptual design, possibly within an optimization algorithm. Symbolic equations of motion of a multibody system are available as a set of ordinary differential equations. Aerodynamic forces are computed based on a rotor effective wind speed at hub height using data tables for thrust and torque coefficients. Hydrodynamic impacts on the floating body are modeled in a way that only the wave height serves as the disturbance signal. This estimation is based on potential flow theory and Morison's formula for slender cylinders. The reduced model code is fully compiled and has a real-time factor of approximately 100. Various simulations of common load cases with a comparison to the certified FAST code have shown to be promising.

1. Introduction

Along with the intensified construction of offshore wind parks worldwide research seeks solutions for seas with a depth beyond the limits of bottom mounted foundations. Several technologies for floating offshore wind turbines (FOWTs) have already been applied in the oil & gas industry. The concepts differ in the way how stability and a reduction of wave excitation is achieved. Tension-leg platforms, for example, achieve stability through taut mooring whereas others, like the barge and spar-buoy, rely on high mass and inertia. The latter is in the focus of this paper: A slender cylinder with a center of gravity far below water level and therefore far below the center of buoyancy. A comparison of these concepts can be found in [2].

The objective of this project is to build a compact simulation tool for a real-time application or a fast conceptual design optimization. A fully coupled simulation of a FOWT requires a combination of structural, aerodynamic and hydrodynamic modules. Various codes exist with a different level of fidelity. The structural module can include complex flexible multibody systems for the wind turbine and the platform with several hundreds of degrees of freedom (DOFs) resulting in computationally expensive systems of differential equations. In terms of hydrodynamics a high fidelity approach is the application of advanced CFD codes. A more generally applicable option is a frequency-domain solution to the separated diffraction, radiation and hydrostatic problem. The connection to the sea-floor via mooring lines also needs to be modeled accurately. Aerodynamics is mostly represented by blade element momentum theory (BEM), which requires iterative algorithms and even higher level CFD models exist, capable of modeling complex aerodynamic effects.

This work, however, aims at a simplified model that reproduces reliably the overall dynamic behavior of the system. Simulation outputs to focus on are, e.g., the unconstrained 3D platform motion, rotor speed, blade pitch angle, tower top displacement and main internal forces. Load distributions or specific node deflections of certain bodies on the other hand are not sought to be covered by the reduced model. This simplification also implies that higher frequency modes of the stiffer DOFs like the blades or generator shaft are not considered. From a numeric point of view focus is set on computational speed so that iterations, recursions, integrations, time-to-frequency domain conversions, excessive memory access, etc. is avoided wherever possible. In order to accomplish these goals the structure is modeled as a coupled multibody system of rigid bodies with only nine DOFs. The equations of motion (EQM) of the 3D model are set up by applying the Newton-Euler formalism. As a result the mathematical model is available in state-space formulation as a system of symbolic ordinary differential equations (ODE) which can be directly compiled, yielding a high computational efficiency. Aerodynamics as well as the mooring line model is based on an interpolation of look-up data that is gained in a pre-processing step. Aerodynamic coefficients allow the calculation of rotor torque and thrust with a scalar rotor-effective wind speed as input. Quasi-static fairlead forces from the mooring lines as a function of horizontal and vertical displacements are stored offline and interpolated during runtime. Hydrodynamic forces are computed by the reduced model through a potential flow approach. Morison's equation is the basis for the herein presented development of a wave load estimation which requires only the current wave height as input. Eventually, kinetics of wave-structure interaction can be calculated without a numerical integration over depth due to the applied deepwater approximation for linear waves.

This paper is structured to first introduce the set-up of the EQM of the structure and then addressing the aero- and hydrodynamic submodels before showing a final comparison to evaluate the code.

2. Wind turbine structural model

Figure 1 shows a sketch of the mechanical model of the OC3-Hywind FOWT, as defined in [3]. A setting with four rigid bodies and nine DOFs has been selected for the reduced model. The EQM will be set up from a physical perspective following the Newton-Euler formalism that is derived in the following sections. The thereby involved operations of matrix algebra are calculated with symbolic programming so that the EQM are finally available as ODEs in a symbolic formulation. The resulting code can then be compiled and thus allows for high flexibility since it can be simulated by standard integration schemes. The next section derives the EQM starting with kinematics and kinetics.

2.1 Kinematics

The multibody system, see fig. 1, consists of the rigid bodies, platform, tower, nacelle and rotor. The total of f DOFs results from the six translational and rotational directions of the platform motion, the translational fore-aft and side-side nacelle displacements and the DOF attributed to the variable rotor speed. These are the generalized coordinates that are comprised in vector $\boldsymbol{q}$. In order to set up Newton's second law for each body i the respective acceleration $\boldsymbol{a}_i$ is needed. It is calculated for scleronomic systems without time-dependent constraints in inertial coordinates as

$$\boldsymbol{a}_i = \dot{\boldsymbol{v}}_i = \boldsymbol{J}_{Ti} \cdot \ddot{\boldsymbol{q}} + \dot{\boldsymbol{J}}_{Ti} \cdot \dot{\boldsymbol{q}} \tag{1}$$

with the translational 3×3 Jacobian matrix $\boldsymbol{J}_{Ti}$ that is the partial derivative of each body's position vector $\boldsymbol{r}_i$ with respect to $\boldsymbol{q}$. Consequently, the total derivative of the Jacobian matrix takes the form

$$\dot{\boldsymbol{J}}_{Ti} = \frac{d}{dt}\frac{\partial \boldsymbol{r}_i}{\partial \boldsymbol{q}}. \tag{2}$$

The formulation corresponding to eqn. (1) for the angular acceleration is

$$\boldsymbol{\alpha}_i = \dot{\boldsymbol{\omega}}_i = \boldsymbol{J}_{Ri} \cdot \ddot{\boldsymbol{q}} + \dot{\boldsymbol{J}}_{Ri} \cdot \dot{\boldsymbol{q}}, \tag{3}$$

where the rotational Jacobian matrix $\boldsymbol{J}_{Ri}$ satisfies the relationship

$$\boldsymbol{\omega}_i = \boldsymbol{J}_{Ri} \cdot \dot{\boldsymbol{q}}. \tag{4}$$

2.2 Multibody system equations

With the accelerations $\boldsymbol{a}_i$ from eqn. (1) and the applied forces and torques $\boldsymbol{f}_i$ and $\boldsymbol{l}_i$ the linear momentum principle of each body is given by

$$\boldsymbol{m}_i \cdot \boldsymbol{a}_i = \boldsymbol{m}_i \cdot (\boldsymbol{J}_{Ti} \cdot \ddot{\boldsymbol{q}} + \dot{\boldsymbol{J}}_{Ti} \cdot \dot{\boldsymbol{q}}) = \boldsymbol{f}_i{}^a + \boldsymbol{f}_i{}^r. \tag{5}$$

Similarly, Euler's law for the angular momentum can be written for body i as

$$\boldsymbol{I}_i \cdot \left(\boldsymbol{J}_{Ri} \cdot \ddot{\boldsymbol{q}} + \dot{\boldsymbol{J}}_{Ri} \cdot \dot{\boldsymbol{q}}\right) + \tilde{\boldsymbol{\omega}}_i \cdot \boldsymbol{I}_i \cdot \boldsymbol{\omega}_i = \boldsymbol{l}_i^a + \boldsymbol{l}_i^r \tag{6}$$

with the inertia tensor $\boldsymbol{I}_i$ and the skew-symmetric matrix $\tilde{\boldsymbol{\omega}}_i$ to the angular velocity $\boldsymbol{\omega}_i$. Eventually, the global equations of motion can be set up through a combination of eqn. (5) and eqn. (6) of all bodies to a system of differential equations. By a multiplication of this resulting equation with the transpose of the global Jacobian $\overline{\overline{\boldsymbol{J}}}^T(\boldsymbol{q})$, which collects all single Jacobian matrices, the reaction forces $\boldsymbol{f}_i^r$ and

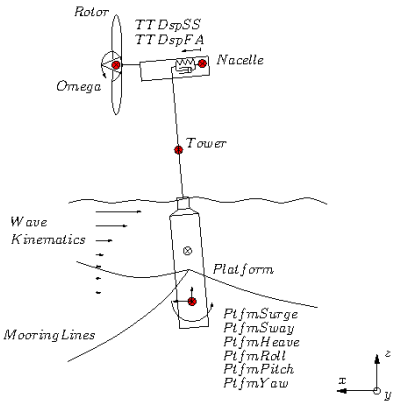

Figure 1 - FOWT mechanical system.

torques $\boldsymbol{l}_i^r$ can be eliminated. Finally, a nonlinear $2f$-dimensional system of first order ODEs according to [4] is obtained,

$$\dot{\boldsymbol{x}} = \begin{bmatrix} \dot{\boldsymbol{q}} \\ \ddot{\boldsymbol{q}} \end{bmatrix} = \begin{bmatrix} \dot{\boldsymbol{q}} \\ \boldsymbol{M}^{-1}(\boldsymbol{p}(\boldsymbol{q},\, \dot{\boldsymbol{q}}) - \boldsymbol{k}(\boldsymbol{q},\, \dot{\boldsymbol{q}},\, \ddot{\boldsymbol{q}})) \end{bmatrix}, \tag{7}$$

with the generalized vector of Coriolis, centrifugal, and gyroscopic forces $\boldsymbol{p}$. The generalized vector of the applied forces $\boldsymbol{k}$ is acceleration-dependent due to the wave-structure interaction, see chapter 4. The next section deals with the calculation of the internal and external applied forces on the plant.

2.3 Kinetics

The only coupling element of the system links the nacelle body to the tower, see fig. 1. The related spring and damping coefficients represent tower bending in fore-aft and side-side direction and are identified through free-decay tests using the certified code FAST [5]. The rotation of the nacelle through tower bending is estimated by a kinematic relationship based on Bernoulli beam theory.

External applied forces $\boldsymbol{f}_i^a$ and torques $\boldsymbol{l}_i^a$, see eqn. (5) and eqn. (6), are coming from the aerodynamics, hydrodynamics and the mooring system. Their derivation in terms of the related submodules is given in the following chapters.

3. Mooring Line Model

The floating platform is moored by three catenary lines that are anchored on the seabed. The differential equation for a stationary line is solved analytically. According to [6] the resulting nonlinear system of equations for the horizontal displacement x_F and the vertical displacement z_F of the fairleads with the corresponding horizontal force H_F and the vertical force V_F has the form

$$\begin{aligned} x_F &= f(H_F, V_F) \\ z_F &= f(H_F, V_F). \end{aligned} \tag{8}$$

Applying a numerical solver the forces on the fairleads can be obtained for various displacements x_F and z_F. Eventually, a function interpolates this data and returns the external forces on the platform body during runtime.

4. Hydrodynamic model

External applied forces from wave-structure interaction can be calculated in various ways. Complex computation uses finite elements so that a flow field around the structure is simulated, giving the pressures over its surface. Simple geometries, like the considered spar-buoy, however, offer the opportunity of applying the well-proven semi-empirical Morison Equation. To apply this equation undisturbed fluid particle kinematics over depth need to be computed through, e.g., potential flow theory, and the resultant force integrated over all structure strips.

For the reduced model the implementation of Morison's formula has specific advantages: First, it is formulated in time-domain which is especially useful for real-time applications. Second, it is independent from multi-dimensional geometry-dependent input parameters and, lastly, there is a valuable means of simplification with the deepwater approximation as explained later in this section. Morison force in both horizontal directions results from an integration of velocity- and acceleration-dependent terms over depth z with water density ρ and cross-sectional area A_X as

$$F_{mor,i} = \rho A_X \int_0^{z_1} (1 + C_A)\, a_{f,i}(t,z) + C_A\, a_{b,i} + C_D\big(u_{f,i}(t,z) + u_{b,i}\big)\big|\boldsymbol{u}_f - \boldsymbol{u}_b\big|\, dz. \tag{9}$$

The coefficient of the added mass term is C_A and the damping coefficient is C_D. Velocities u_i and accelerations a_i have an index f if they refer to fluid particles and an index b if they refer to body velocities. This dependency on structure accelerations yields the implicit formulation of eqn. (7). The functions that describe fluid particle kinematics over depth derived from potential flow theory in both horizontal directions are hyperbolic. For the velocity potential Φ of the fluid over depth in x-direction remains with the free-surface elevation η and gravity constant g for draft length h

$$\Phi(z,\eta,\omega) = \frac{g}{\omega}\frac{\cosh[k(z+h)]}{\cosh(kh)}\eta. \tag{10}$$

This function depends on the wave angular frequency ω and the wavenumber k that is itself related to the wave frequency through the implicit dispersion relationship, see [1].

The frequency-dependency of the model is a challenge regarding a real-time implementation, since the wave frequency is not easily measurable. Another issue of eqn. (10) is that it cannot be integrated analytically over the water depth z and requires a numerical loop that would significantly slow down the code. In order to solve these issues the velocity potential Φ is rewritten using deepwater approximation so that the potential

$$\Phi^{dw}(z,\eta,\omega) = \frac{g}{\omega} e^{kz}\eta \tag{11}$$

remains according to [1] as a simple exponential function. This simplifies eqn. (9) considerably if its last term, the vectorial contribution is neglected. That term is a correction to Morison's original formula, see [7], for differing spatial directions between fluid and structure motion. With the fluid kinematics described as exponentials rather than hyperbolic functions it is possible to integrate eqn. (9) over depth z analytically rather than through a numeric loop and therefore save computational time. If the wave angular frequency ω is additionally available further useful reduction of the wave disturbance model is achieved. This information might come from sensor measurements or an estimation, for example as the peak angular frequency ω_p of the wave spectrum. Thus, the fluid kinematics as input to Morison's equation (10) are no longer necessary but only the free-surface elevation η, which is easily measurable. Consequently, a method is presented to compute wave loads on the spar-buoy in real-time using deepwater approximation to the linear potential flow theory estimating a peak spectral wave frequency. For the external force from aerodynamics a similarly simple model with measurable inputs has been developed as given in the following.

5. Aerodynamic model

Lift and drag forces on the rotor blades can be calculated through complex computational methods that simulate a turbulent wind field and output fluid-structure forces on the blades. BEM theory as industry standard relates a three-dimensional wind field to lift and drag forces on blade elements. However, this method requires an iteration to find the induction factors, which is correlated with a high numerical effort. This will be avoided for the reduced model by simulating Aerodyn's BEM model, see [8], for various tip-speed ratios λ and blade pitch angles Θ until a steady state is reached as a pre-processing step. With the resulting two-dimensional look-up table for the thrust and torque coefficients c_T and c_P only the rotor effective wind speed is necessary to calculate the thrust force F_{aero} and torque M_{aero} on the rotor. In order to compute this representative wind speed at hub height first, a weighted average of the three-dimensional turbulent wind field on the whole rotor plane is needed, given by v_0. Second, a transformation of this estimation into the rotor coordinate system is necessary, so that the relative horizontal wind speed is computed. Finally, the relative rotor effective wind speed takes the form

$$v_{rel} = \dot{r}_{rotor,x} - v_0. \tag{12}$$

This is the scalar disturbance necessary to calculate the thrust force

$$F_{aero} = \frac{1}{2}\rho\pi R^2 c_T(\lambda,\Theta) v_{rel}^2 \tag{13}$$

and the external aerodynamic torque acting on the rotor body

$$M_{aero} = \frac{1}{2}\rho\pi R^3 \frac{c_P(\lambda,\Theta)}{\lambda} v_{rel}^2 \tag{14}$$

with air density ρ and rotor radius R. The described method has already been tested and successfully implemented for nonlinear model predictive control (NMPC) in [9].

To account for yawed or pitched oblique inflow various simulations with the code Aerodyn [8] have been performed. It could be shown that the

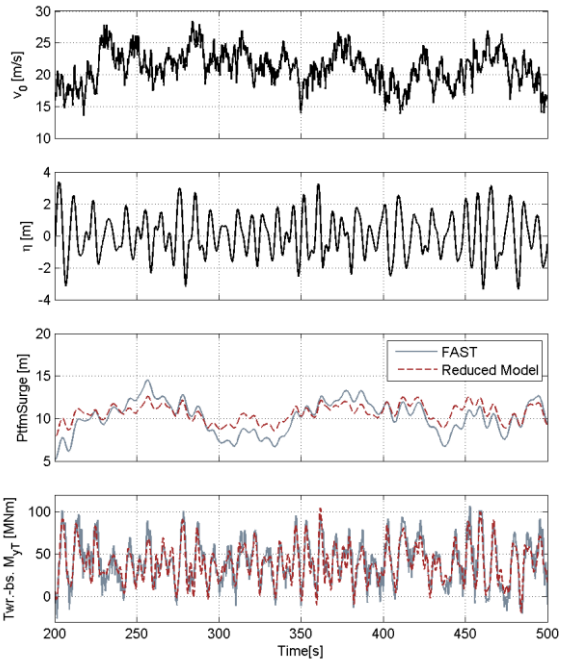

Figure 1 – Platform surge displacement and tower base moment at turb. wind with mean wind $v_0 = 20\ \mathrm{m/s}$, irregular waves with significant wave height $H_s = 6\ \mathrm{m}$ and peak spectral period $T_p = 10\ \mathrm{s}$.

magnitude of the thrust force F_{aero} and torque M_{aero} varies proportionally to the cosine of the angle of inflow. However, the applied BEM model also returns an eccentric location of the resultant thrust force on the rotor which is neglected for the reduced model.

6. Reduced model evaluation

In order to estimate the validity of the built model various simulations have been performed with the certified FAST code [5] and the reduced model. FAST is an aero-hydro-servo-elastic code with a modal reduction of the structure up to the 2nd modes and a total of 22 DOFs. The hydrodynamic model uses linear potential flow theory with the radiation and diffraction solution and aerodynamics based on BEM theory. First evaluations from a free-decay test with constant wind from an upright platform position have returned good results in terms of frequency, ratio of decay and steady states.

Realistic simulations with turbulent wind and irregular waves give the results shown in fig. 1. Wind and wave disturbances can be seen on top and timeseries of platform surge displacement and tower base pitching moment M_{yT} below. The platform surge displacement shows deviations for low frequencies, which come from the estimation of the peak spectral period as mentioned in chapter 4. The internal tower base bending moment is a good measure for model evaluation since it includes all applied mass and inertia forces of the wind turbine. Its time-domain plot shows a good agreement for the applied boundary conditions.

Figure 2 shows the power spectral density function (PSD) of moment M_{yT} for the two models. The first peaks of the PSD, being the platform pitch

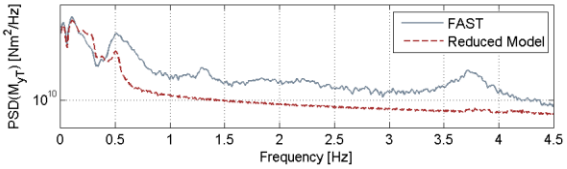

Figure 2 – PSD of tower base pitching moment.

eigenfrequency, the peak spectral wave frequency and the first tower eigenfrequency, coincide. Higher frequencies are not represented by the reduced model. The reliability and fidelity of the model for conceptual design purposes has been evaluated within a statistical study with FAST as reference for various IEC load cases, see [10].

7. Conclusion and outlook

The objective of this work was to build a fast standalone numerical model of a spar-mounted FOWT that reliably reproduces the overall behavior of the system. A real-time factor of about 100 is achieved by simplifying physical models and avoiding numerical loops. Steady states, resonance frequencies up to the first tower mode and a statistical analysis of IEC load cases confirm the validity of the model. In a next step it will be used as an internal model for NMPC and design optimization. Further extensions will aim at improving the accuracy of the aerodynamic model for e.g. yawed inflow and the hydrodynamic model for non-slender bodies.

References

[1] M. E. McCormick, *Ocean Engineering Mechanics*. Oxford University Press, 2010.

[2] D. Matha, “Model Development and Loads Analysis of an Offshore Wind Turbine on a Tension Leg Platform with a Comparison to Other Floating Turbine Concepts,” 2009.

[3] J. Jonkman, “Definition of the Floating System for Phase IV of OC3,” 2010.

[4] W. Schiehlen and P. Eberhard, *Technische Dynamik - Modelle für Regelung und Simulation*. Stuttgart: B.G. Teubner, 2004.

[5] J. Jonkman and M. L. Buhl, “Fast User’s Guide.” Aug-2005.

[6] J. Jonkman, “Dynamics Modeling and Loads Analysis of an Offshore Floating Wind Turbine,” 2007.

[7] J. R. Morison, “The Force Distribution Exerted by Surface Waves on Piles,” 1953.

[8] A. C. Hansen and D. J. Laino, “User’s Guide to the Wind Turbine Aerodynamics Computer Software AeroDyn.”

[9] D. Schlipf, D. J. Schlipf, and M. Kühn, “Nonlinear Model Predictive Control of Wind Turbines Using LIDAR,” *Wind Energy*, 2012.

[10] D. Matha, F. Sandner, and D. Schlipf, “Efficient Critical Design Load Case Identification for Floating Offshore Wind Turbines with a Reduced Nonlinear Model,” in *The Science of Making Torque from Wind*, 2012.